THE JOURNAL OF BIOLOGICAL CHEMISTRY VOL. 290, NO. 21, pp. 13042–13052, May 22, 2015

Abscisic Acid Transport in Human Erythrocytes*

Received for publication, December 1, 2014, and in revised form, March 3, 2015 Published, JBC Papers in Press, April 6, 2015, DOI 10.1074/jbc.M114.629501

Tiziana Vigliarolo[‡1], Lucrezia Guida[‡], Enrico Millo[§], Chiara Fresia[‡], Emilia Turco[¶], Antonio De Flora[‡], and Elena Zocchi[‡]

From the [‡]Department of Experimental Medicine, Section of Biochemistry, and the [§]Center of Excellence for Biomedical Research, University of Genova, Genova 16132, Italy and the [¶]Department of Molecular Biotechnology and Health Sciences, University of Torino, Torino 10126, Italy

Background: The plant stress hormone abscisic acid (ABA) is present and active in mammalian cells.
Results: Band 3 protein is required for ABA influx into red blood cells (RBC); intracellular ABA activates adenylate cyclase resulting in $[cAMP]_i$ increase and subsequent ATP release.
Conclusion: ABA influx through Band 3 activates ATP release from RBC.
Significance: Paracrine ABA may regulate the ATP-mediated vasodilator response to inflammation.

Abscisic acid (ABA) is a plant hormone involved in the response to environmental stress. Recently, ABA has been shown to be present and active also in mammals, where it stimulates the functional activity of innate immune cells, of mesenchymal and hemopoietic stem cells, and insulin-releasing pancreatic β-cells. LANCL2, the ABA receptor in mammalian cells, is a peripheral membrane protein that localizes at the intracellular side of the plasma membrane. Here we investigated the mechanism enabling ABA transport across the plasmamembrane of human red blood cells (RBC). Both influx and efflux of [^{3}H]ABA occur across intact RBC, as detected by radiometric and chromatographic methods. ABA binds specifically to Band 3 (the RBC anion transporter), as determined by labeling of RBC membranes with biotinylated ABA. Proteoliposomes reconstituted with human purified Band 3 transport [^{3}H]ABA and [^{35}S]sulfate, and ABA transport is sensitive to the specific Band 3 inhibitor 4,4′-diisothiocyanostilbene-2,2′-disulfonic acid. Once inside RBC, ABA stimulates ATP release through the LANCL2-mediated activation of adenylate cyclase. As ATP released from RBC is known to exert a vasodilator response, these results suggest a role for plasma ABA in the regulation of vascular tone.

Abscisic acid (ABA)[2] is a plant hormone regulating several important functions in higher plants, including response to abiotic stress, control of stomatal closure, and regulation of seed germination (1, 2). In plants, several ABA receptors with different cellular localizations have been identified (3). Recent studies identified PYR/PYL/RCAR proteins as ABA receptors that are localized in the cytosol and nucleus (4, 5). Because PYR/PYL/RCAR are intracellular soluble receptors and ABA may be produced by cell types different from those that are functionally responsive to the hormone, ABA transport across the cell membranes is necessary to the action of the hormone. Indeed, several ABA transporters have been recently identified in plants. Two members of the ATP-binding cassette (ABC) transporter family, AtABCC25 and AtABCG40, were found to function as ABA transporters (6, 7) and another type of ABA transporter, AIT1/NRT1.2 (nitrate transporter family), was identified as an ABA influx facilitator (8). These transporters are involved in ABA efflux and influx with tissue-specific expression. Very recently, an *Arabidopsis* DTX/MATE family member, DTX50, has been shown to function as a mediator of ABA efflux (9).

Several reports have demonstrated that ABA is present and functionally active in a wide range of animals, from lower Metazoa to a variety of mammalian tissues and cells (10, 11). In human granulocytes and other cells of the innate immune response, ABA stimulates cell-specific functions, such as phagocytosis, chemotaxis, reactive oxygen species, and nitric oxide production (12–14). ABA also expands human mesenchymal stem cells (15) and human hemopoietic progenitors (16). In cells involved in the control of systemic glucose homeostasis, ABA is an endogenous stimulator of insulin release from pancreatic β cells and an enhancer of glucose uptake by adipocytes and myoblasts (17). It was previously suggested that the lanthionine synthetase C-like protein 2 (LANCL2) is required for ABA binding to the plasma membrane of granulocytes and is necessary for the transduction of the ABA signal in granulocytes and in rat insulinoma cells (18). More recently, docking studies predicted (19), and experiments with the recombinant protein demonstrated (20), ABA binding to LANCL2. The LANCL2 protein is associated with the plasma membrane through N-terminal myristoylation and a basic phosphatidylinositol phosphate-binding site (21). However, protein lipidation, a typical feature of peripheral membrane proteins, has been recently observed in integral membrane proteins as well (22), and previous immunofluorescence studies performed on LANCL2-overexpressing cells were inconclusive regarding the transmembrane or peripheral position of LANCL2 (18). Here, we investigated LANCL2 localization in human erythrocytes,

* This work was supported in part by the Italian Ministry of Education, University and Scientific Research Grant PRIN 2007BZ4RX3_005, the Fondazione CARIGE, and the Compagnia di S. Paolo di Torino (ID ROL 316).
[1] To whom correspondence should be addressed: Dept. of Experimental Medicine, Section of Biochemistry, University of Genova, Viale Benedetto XV 1, Genova 16132, Italy. Tel: 390103538158; Fax: 3901035338162; E-mail: tiziana.vigliarolo@edu.unige.it.
[2] The abbreviations used are: ABA, abscisic acid; LANCL2, lanthionine synthetase C-like protein 2; mAb LANCL2, monoclonal anti-LANCL2 antibody; bio-ABA, biotinylated abscisic acid; OG, β-octyl glucopyranoside; DIDS, 4,4′-diisothiocyanostilbene-2,2′-disulfonic acid; AC, adenylate cyclase; HBSS, Hanks' balanced salt solution.

and found that LANCL2 is a peripheral protein attached to the intracellular side of the RBC membrane; thus, for ABA to enter into RBC and bind to its receptor, ABA transport across the plasma membrane is necessary. We further provide direct evidence, by different methodological approaches, that the transmembrane anion exchange protein Band 3 mediates ABA influx into erythrocytes and that extracellular ABA stimulates ATP release from intact RBC via LANCL2-mediated adenylate cyclase activation.

Experimental Procedures

Materials—(*R*,*S*)-[^{3}H]Abscisic acid ([^{3}H]ABA) was purchased from Biotrend Radiochemicals, Köln, Germany (20 Ci/mmol), [^{3}H]NAD$^+$ (25 Ci/mmol) and [^{35}S]sulfate (755 mCi/mmol) were obtained from PerkinElmer Life Sciences (Milan, Italy).

Biotinylated abscisic acid (bio-ABA) was synthesized from (±)2-cis, 4-trans abscisic acid by coupling (+)-biotin-ϵ-aminocaproyl hydrazide to the carbonylic group on the ABA carbon ring via an ϵ-aminocaproyl hydrazide linker, as described in Ref. 23. All chemicals were obtained from Sigma (Italy). ABA was dissolved in H_2O at a concentration of 50 mM, the pH was adjusted to 7.4 with NaOH or dissolved in Tris-HCl, 0.1 M, pH 7.4, at a concentration of 50 mM and the stock solutions were kept at −20 °C.

Preparation of a Monoclonal Antibody against Human LANCL2—The monoclonal antibody (mAb) against LANCL2 was obtained at the Molecular Biotechnology Center (MBC) in Torino (Italy), by fusing myeloma cells (NS1) with the spleen cells from a mouse immunized with the recombinant fusion protein LANCL2-GST obtained in *Escherichia coli* (20). One subclone was selected for its high specificity (*i.e.* no cross-reactivity toward the homolog LANCL1 protein), and best sensitivity for Western blotting, immunoprecipitation, and ELISA applications on various cell lysates.

The anti-LANCL2 mAb was affinity purified from ascites fluid or from the medium of cultured hybridoma cells on protein A-Sepharose, as described previously (24). Bound antibodies were eluted with 0.1 M glycine, pH 3, and dialyzed against PBS. Stock solutions of mAb at 2 and 0.2 mg/ml in PBS were kept at 4 °C.

Preparation of Erythrocyte Membranes (White Ghosts)—Freshly drawn blood samples were obtained from healthy human volunteers. Washed, packed erythrocytes were hemolyzed in 10 volumes of ice-cold 5 mM sodium phosphate (Na_2HPO_4, hypotonic buffer), pH 8.0, containing 80 μg/ml of PMSF and 2 mM EDTA, and centrifuged at 15,000 × *g* for 20 min at 4 °C. Erythrocyte ghosts were further washed several times in 10 volumes of the same buffer, to obtain complete removal of hemoglobin, and once in deionized H_2O. The final pellet was resuspended at 1 mg/ml in H_2O and used directly or kept frozen at −20 °C. Protein assays were performed according to Bradford (25). White ghosts were resealed as described in Ref. 26.

Stripping of Peripheral Proteins from Ghosts and Western Blot—Extrinsic proteins were removed from 1 ml of white ghosts at 1 mg/ml by sequential washing with the following ice-cold buffers: (i) once with 10 volumes of 2 mM EDTA, pH 12; (ii) three times with 10 volumes of 1 M KI, and (iii) once with water. After each washing, the membranes were centrifuged at 4 °C, 100,000 × *g* for 10 min; finally, pellets were resuspended at 1 mg/ml in H_2O. In the experiments for LANCL2 localization in ghosts, supernatants were collected and concentrated with an Amicon Ultra, Ultracel 30k (Millipore, Milan, Italy). LANCL2 protein expression was determined by Western blot using the monoclonal antibody against LANCL2 (see above): after SDS-PAGE, performed according to the standard method on 10% gels, proteins were transferred to a 0.2-μm nitrocellulose membrane (Bio-Rad). Blots were probed with a primary LANCL2 mouse monoclonal antibody and a secondary anti-mouse IgG antibody conjugated with horseradish peroxidase (HRP) (Santa Cruz Biotechnology) and developed with Immobilon™ Western Chemiluminescent HRP Substrate (Millipore). Detection and densitometry were performed using a Chemi-Doc System (Bio-Rad).

Transport Assay in Erythrocytes—Fifty-μl aliquots of RBC at a 5% hematocrit in Hanks' balanced salt solution (HBSS) were incubated at 22 °C in triplicate with 3.5, 7, 14, 28, 56, 114, 200, and 300 nM [^{3}H]ABA for 30 s with 100 nM [^{3}H]ABA or, for the time course experiments, with 200 nM [^{3}H]ABA for 0.5, 3, 5, 15, 30, and 60 min. After incubation, RBC were washed 3 times in ice-cold HBSS. In the experiments with chloride-free buffer, RBC were washed 4 times with sodium citrate buffer (80 mM Na-citrate, pH 7.4). The cells were resuspended at a 5% hematocrit in HBSS or in citrate buffer and were incubated with 200 nM [^{3}H]ABA or 3.5 μM [^{35}S]sulfate for 5 min in the presence or absence of 100 mM NaCl.

RBC were then centrifuged for 15 s at 16,000 × *g*, the supernatants were discarded and the cell pellets were washed once with 1.5 ml of ice-cold HBSS or citrate buffer. Cells were resuspended in 200 μl of 5.5 M H_2O_2 and after 18 h the radioactivity of the samples was determined after addition of 5.0 ml of Ultima-Gold (PerkinElmer Life Sciences, Milan, Italy) using a Packard β-counter (Beckman-Coulter, Krefeld, Germany).

To evaluate ABA efflux from RBC, cells were incubated at 22 °C at a 5% hematocrit in HBSS buffer in 50 μl final volume at 22 °C in triplicate for 30 min with 200 nM [^{3}H]ABA. The pellets were then washed with 1.5 ml of HBSS for 4 times at 37 °C. Intracellular radioactivity was estimated as described above.

HPLC—Fifty-μl aliquots of RBC at a 50% hematocrit were incubated in duplicate for 30 s in 50 μl of HBSS with 0.025, 0.25, 2.5, 10, and 25 mM ABA. Cells were washed twice with 1.6 ml of ice-cold HBSS, resuspended in 100 μl of H_2O, extracted with 4 volumes of ice-cold acetone and stored at −20 °C. The extracts were centrifuged for 5 min at 16,000 × *g*, and after removal of acetone from the supernatants, the aqueous extract was acidified at pH 2.6 with trifluoroacetic acid and extracted with diethyl ether (27). After removal of diethyl ether under a nitrogen flux the extract was re-dissolved in H_2O and subjected to HPLC analysis with a Hewlett-Packard HP1200 instrument. The column was an Atlantis C18 (3.9 × 150 mm, 5 μm, Waters, Milan, Italy): solvent A was H_2O containing 0.01% (v/v) acetic acid, solvent B was 100% acetonitrile. The solvent program was a linear gradient (at a flow rate of 0.8 ml/min) starting at 100% solvent A and increasing to 100% solvent B in 30 min. ABA was detected with an HP 1040 diode array spectrophotometric

detector set at 260 nm: ABA was eluted at 17.5 min. Peak areas of sample ABA were compared with those of a computer-stored standard, allowing both identification and quantification of the hormone.

Screening of Inhibitors—The various compounds were dissolved in dimethyl sulfoxide and stored at −20 °C as 100 mM stock solutions. For transport assay, RBC at a 5% hematocrit in HBSS buffer were preincubated for 30 min at 37 °C with the compounds at a final concentration of 100 μM containing 0.1% dimethyl sulfoxide, then RBC were centrifuged (15 s at 16,000 × *g*), and pellets were washed once with 1.6 ml of ice-cold HBSS. Cells were resuspended at a 5% hematocrit and incubated with 200 nM [^{3}H]ABA for 5 min. After washing, the intraerythrocytic ABA concentration was estimated by counting the cell radioactivity.

Purification of Bio-ABA-binding Proteins—A volume of 300 μl of resealed ghosts (1 mg/ml) was incubated with 100 μM bio-ABA in the presence or absence of excess unlabeled ABA (10 mM) for 3 h and the membranes were irradiated with UV light (0.4 Joules) for 5 min. After UV irradiation, the membranes were centrifuged for 10 min at 100,000 × *g* at 4 °C and the pellets were washed once with ice-cold PBS by centrifugation and solubilized in lysis buffer (150 mM NaCl, 50 mM Tris-HCl, pH 7.4, 1% Nonidet P-40) with a protease inhibitor mixture for mammalian cells (Sigma). A volume of 300 μl of magnetic streptavidin-coated beads (10 mg/ml, binding capacity: 600 pmol biotin/mg resin, FLUKA, Italy) was washed 3 times with isotonic buffer (150 mM NaCl, 10 mM Tris-HCl, 1 mM $CaCl_2$, 0.2 mM EDTA) and incubated with the solubilized samples overnight at 4 °C with mild shaking. Then, the beads were washed 3 times with isotonic buffer, resuspended in Laemmli sample buffer, and heated for 5 min at 99 °C. The supernatant was collected and the bio-ABA-binding proteins were analyzed by SDS-PAGE and Western blot using an anti-streptavidin-HRP antibody; gels were stained with ProSieve Blu Protein Staining solution (Lonza, Italy). Blots were also probed with a primary mAb against Band 3 (Santa Cruz Biotechnology) and a secondary anti-mouse IgG-HRP antibody.

Reconstitution of Purified Band 3 into Liposomes—Native Band 3 was purified from white ghosts after stripping of peripheral proteins, as described above. The stripped ghosts (1 mg/ml in H_2O) were incubated for 10 min at 4 °C with 1% (w/v) β-octyl glucopyranoside (OG) (Sigma). After centrifugation at 100,000 × *g* for 10 min at 4 °C, the supernatants were supplemented with 1/10 (v/v) of 400 mM K_2HPO_4, pH 7.5, and applied directly to a diethylaminoethyl-cellulose (DE-52 preswollen microgranular, Whatman, Dassel, Germany) anion exchange column (0.6 ml of resin/mg of solubilized protein) pre-equilibrated with 40 mM K_2HPO_4, pH 7.5, containing 0.5% OG (DE-52 buffer). The column was washed with 3 column volumes of DE-52 buffer and then with 3 volumes of 0.15 M NaCl, 0.15 M K_2HPO_4, pH 7.5, containing 0.5% OG, which removed the majority of contaminant proteins. Band 3 was eluted with 1 M NaCl (step 1) and with 1.5 M NaCl (step 2), both containing 0.15 M K_2HPO_4, pH 7.5, and 0.5% OG. The fractions eluted from the column were subjected to protein assay and SDS-PAGE (10% polyacrylamide gels) was performed after dialysis in isotonic buffer and concentration of the fractions with Amicon Ultra. Western blot was performed on 1–2 μg of the fractions with a primary mAb against Band 3 and a secondary anti-mouse IgG-HRP antibody.

The liposomes and proteoliposomes were composed of total lipids extracted from erythrocyte membranes as described in Ref. 26. Briefly, the dried lipids film (0.8–1 mg) was mixed with 2 ml of the proteins eluted from the DE-52 at 1 M NaCl, 0.15 M K_2HPO_4, pH 7.5 (protein concentration range, 8 to 10 μg/ml, proteo-1), and at 1.5 M NaCl, 0.15 M K_2HPO_4, pH 7.5 (protein concentration range, 0.6 to 1.2 μg/ml, proteo-2), both containing 1% OG (final concentration). The resulting emulsions were vortexed and sonicated 30 s on ice for 3 times. The sonicated solutions were extensively dialyzed against 5 liters of isotonic buffer for 42 h at 4 °C. Control liposomes were prepared without the addition of any protein. After dialysis the liposomes and proteoliposomes were centrifuged at 100,000 × *g* for 10 min at 4 °C, and the pellets were resuspended in 0.3 ml of isotonic buffer. The total lipids in the proteoliposome and liposome were determined on 5–10-μl aliquots, as described (26), and proteins were determined after addition of 1% Triton X-100 in 10–100 μl, using the Lowry assay (28).

Transport Assays in Liposomes and in Band 3-reconstituted Proteoliposomes—To test ABA transport in liposomes and proteoliposomes, proteo-2 and control liposomes were incubated in isotonic buffer at 22 °C with 100 nM [^{3}H]ABA from 0 to 30 min for the time course experiments, or for 30 min, with 500 nM [^{3}H]ABA, 500 nM [^{3}H]NAD^+, or 3.5 μM [^{35}S]sulfate. To inhibit Band 3 transport, ghosts were preincubated without (control) or with 100 μM DIDS (Sigma) that was dissolved at 1 mM concentration with 0.1 M $KHCO_3$ for 30 min at 37 °C and then centrifuged once at 100,000 × *g*. Pellets were resuspended at 1 mg/ml in 40 mM K_2HPO_4, pH 7.5, with 1% OG. Band 3 was purified and proteoliposomes were obtained as described above. Transport assays were performed by incubating the proteoliposomes with 100 nM [^{3}H]ABA or 3.5 μM [^{35}S]sulfate for 30 min. At the various time points, 50-μl aliquots (each sample was assayed in triplicate) were filtered on a glass fiber paper (GF/C Whatman™). Filters were washed with 3 ml of isotonic buffer on ice, dried, and the radioactivity was determined using a Packard β-counter.

Determination of Intracellular cAMP Levels—RBC were resuspended in HBSS at a 50% hematocrit and preincubated for 15 min with 250 μM cAMP phosphodiesterase inhibitor 3-isobutyl-1-methylxanthine (Sigma). Then, duplicate 500-μl aliquots were incubated for 5 min without (control) or with 10 μM ABA, in the absence or presence of 10 μM analog #10 (29), or 100 μM DIDS (stock solution was dissolved in 0.1 M $KHCO_3$ at a concentration of 1 mM). The intracellular cAMP concentration was determined by RIA, as described (12).

Determination of ATP Release from RBC—Washed erythrocytes were diluted to a 0.05% hematocrit in HBSS. The extracellular ATP concentration was determined with an ATP determination kit (Invitrogen), following the manufacturer's instruction.

A 250-μl sample of erythrocyte suspension at a 0.05% hematocrit was incubated without or with 0.1, 1, and 100 μM ABA for 20 min at 22 °C. Cells were then centrifuged for 30 s at

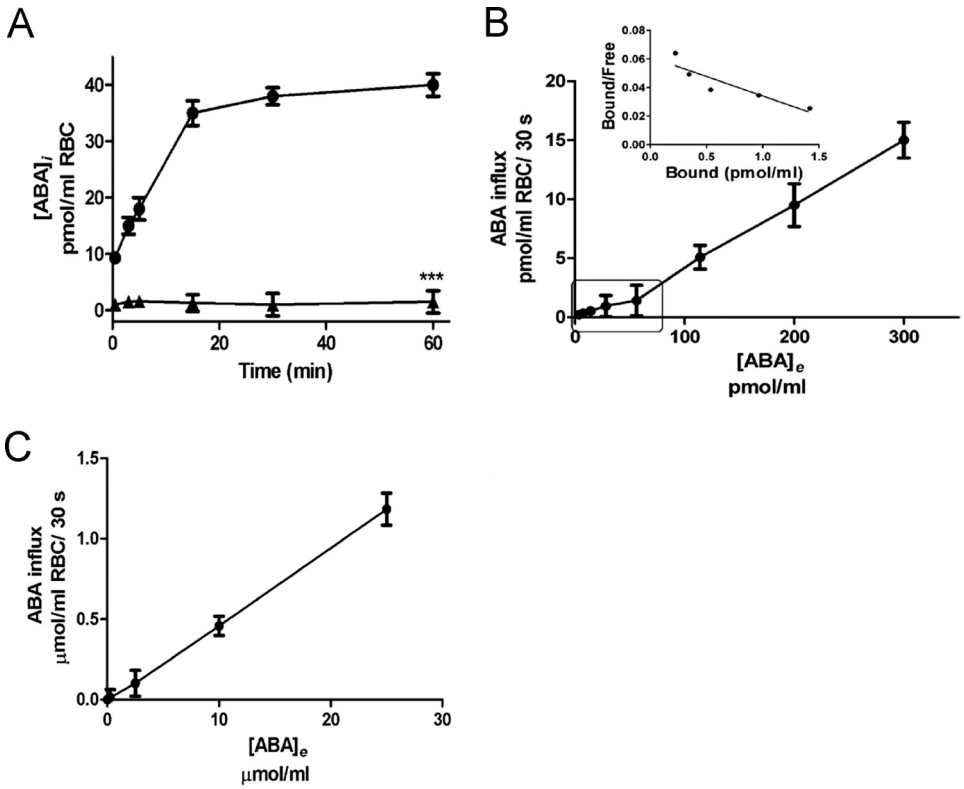

FIGURE 1. **ABA influx into human RBC.** *A*, RBC were incubated at a 5% hematocrit with 200 nM [^{3}H]ABA for 0.5, 3, 5, 15, 30, and 60 min at 22 °C (*circles*) or 0 °C (*triangles*). At various time points, incubation aliquots were centrifuged, cells were washed at 0 °C, and the intracellular radioactivity was counted as described under "Experimental Procedures." ***, $p < 0.001$ for all points of the curve. *B*, RBC were incubated in HBSS at a 5% hematocrit for 30 s at 22 °C with 3.5, 7, 14, 28, 56, 114, 200, and 300 nM [^{3}H]ABA. Intracellular ABA was estimated after washing RBC pellets and counting the radioactivity. The *inset* shows the Scatchard plot of [^{3}H]ABA from 3.5 to 56 nM. *C*, RBC were incubated at a 50% hematocrit with 0.025, 0.25, 2.5, 10, and 25 mM unlabeled ABA. Intracellular ABA concentrations were determined on deproteinized cell extracts by HPLC analysis, as described under "Experimental Procedures."

16,000 × *g* and 20 μl of the supernatants were added to 180 μl of reaction buffer in each well of a 96-well plate.

Luminescence was measured using a FLUOstar OPTIMA (BMG Labtech, Ortenberg, Germany). ATP concentrations in the experimental samples were calculated from the ATP standard curve.

Statistical Analysis—Data were compared by means of the Student's unpaired *t* test, or one-way analysis of variance. Statistical significance was set at $p < 0.05$. Statistical analysis was performed using the GraphPad Prism Software (GraphPad Software Inc.).

Results

ABA Binding and Influx into Erythrocytes—Previous experiments of [^{3}H]ABA binding to intact human granulocytes (12) had revealed two processes characterized by different affinity constants: (i) a high affinity binding (K_d = 11 nM), which was interpreted as ABA binding to receptor and (ii) a low affinity binding (K_d = 500 μM), which was interpreted as ABA interacting with intracellular proteins, after influx into the cells.

First we examined some general properties of ABA uptake by intact RBC. ABA influx occurred over a pH range from 6.7 to 8.0, with a 50% decrease at pH 8.0 compared with pH 6.7. Transport was reduced by 90% in RBC pre-treated with 1% glutaraldehyde and was completely abrogated at 0 °C. No appreciable variation of ABA influx was observed over a temperature range between 20 and 37 °C. Therefore, ABA transport was analyzed at 22 °C and at pH 7.4. The time course of ABA influx in RBC is shown in Fig. 1*A*. When RBC were exposed to 200 nM [^{3}H]ABA, a rapid uptake occurred within the first 15 min and intraerythrocytic concentrations remained stable thereafter for up to 60 min.

Next, RBC were incubated in HBSS with increasing concentrations of extracellular [^{3}H]ABA, and the initial rate of ABA uptake was measured. As shown in Fig. 1*B*, at low [^{3}H]ABA concentrations (3.5 to 56 nM), a saturable binding was observed and the Scatchard plot analysis indicated the presence of high affinity binding sites (K_d = 52 nM). These results could be attributed to the interaction between ABA and its receptor LANCL2, which is expressed in erythrocytes, as demonstrated below. Conversely, at higher [^{3}H]ABA concentrations (100 to 300 nM), an apparently non-saturable process was observed (Fig. 1*B*). RBC were thus incubated with unlabeled ABA at concentrations up to 25 mM and the intracellular ABA was determined by HPLC analysis (Fig. 1*C*). Saturation of the transporter was still not observed up to the highest ABA concentration tested (25 mM). Increasing the extracellular ABA concentration above this value was not possible due to its insolubility in neutral aqueous solutions (the maximal concentration attainable being ~50 mM). Thus saturation of the transporter requires ABA concentrations higher than 25 mM.

LANCL2 Localization in Ghosts—As ABA binding and transport co-exist in RBC, we addressed the question whether

LANCL2 could function as an ABA transporter, in addition to its established role as ABA receptor (18, 20). Previous experiments of immunofluorescence labeling of LANCL2, fused with the C-terminal V5 peptide, with an anti-V5 antibody (18), demonstrated that in transfected $CD38^+/LANCL2^+$ HeLa cells LANCL2 localizes at the plasma membrane, although it was not clear whether as an intrinsic or peripheral protein. To identify LANCL2 localization, we subjected erythrocyte ghosts to high ionic strength and alkaline pH in the absence of detergents to remove the peripheral proteins. After treatment, the ghost pellets, containing transmembrane proteins, and the supernatant, containing the concentrated peripheral proteins, were analyzed by SDS-PAGE. Fig. 2 shows a representative Western blot, probed with a monoclonal anti-LANCL2 antibody (mAb LANCL2). LANCL2 was mainly present in the supernatant and only traces of the protein were visible in the membrane pellets after chemical treatment. The fact that LANCL2 can be removed from the ghosts by simply increasing ionic strength and pH demonstrates that LANCL2 is not an integral protein. This result indicates that LANCL2 cannot be involved in the direct passage of ABA across the plasma membrane.

Properties of ABA Transport in RBC—To investigate other properties of ABA transport, RBC were loaded with 200 nM [^{3}H]ABA and then submitted to 4 sequential washings at 0 or 37 °C with 1.5 ml of HBSS. Because the ABA content in the RBC washed at 37 °C was significantly lower compared with that in RBC washed at 0 °C (Fig. 3*A*), we conclude that ABA transport in RBC is equilibrative, allowing movement of ABA across the plasma membrane down a concentration gradient.

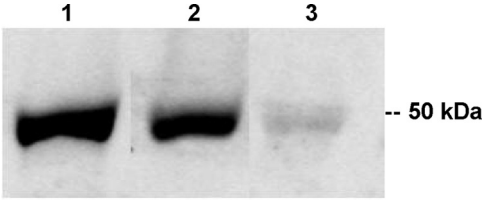

FIGURE 2. **LANCL2 is a peripheral protein in ghosts.** Twenty μg of white ghosts were washed to remove extrinsic proteins as described under "Experimental Procedures." White ghosts before treatment (*lane 1*), the concentrated supernatants from the washings, containing the extrinsic proteins (*lane 2*), and the washed pellets, containing integral proteins only (*lane 3*) were analyzed by Western blotting using an anti-LANCL2 monoclonal antibody.

Next, we addressed whether the extracellular ABA uptake was affected by specific inhibitors of selected transport systems known to be present in RBC (Fig. 3*B*). Each of these inhibitors was used at a final concentration of 100 μM. Concerning the ATP-dependent transport systems, ABA influx was unaffected either by ouabain, an inhibitor of the Na^+/K^+-ATPase, or by verapamil, indomethacin, or glibenclamide, all inhibitors of the ATP binding cassette transporters multidrug resistance protein 1 (MDRP1), and cystic fibrosis transmembrane conductance regulator. As far as the mechanisms of facilitated diffusion present in the erythrocytes are concerned, the inhibitors of the nucleoside transporter and the glucose transporter were ineffective. Instead, DIDS, an inhibitor of the anion exchanger Band 3, and also of other membrane transporters expressed in nucleated cells, including Na,K-ATPase (30, 31), Ca^{2+}-ATPase (32), and canalicular bile salt transport system (33), reduced ABA uptake by 70%. We also tested DIDS at a final concentration of 500 μM, in the absence or presence of 2.5 mM ABA for 5 min. ABA influx into RBC, as measured by HPLC analysis, was inhibited by ~90%.

DIDS is also an irreversible inhibitor of the monocarboxylic acids transporter (MCT-1) (34). Because the MCT-1-specific inhibitor AR-C155858 at 100 μM had only a limited inhibitory effect on ABA influx (10%), a major role of MCT-1 in ABA transport in RBC is unlikely (Fig. 3*B*). These results suggest that Band 3 is the major contributor to ABA transport in RBC. ABA is a weak organic acid ($pK = 4.8$); protonated ABA (ABA-COOH) is the main form at low pH, whereas de-protonated ABA ($ABA\text{-}COO^-$) prevails at pH > 4.8. Thus, at physiological pH (around 7.4), de-protonated ABA is the predominant form of the hormone transported by Band 3.

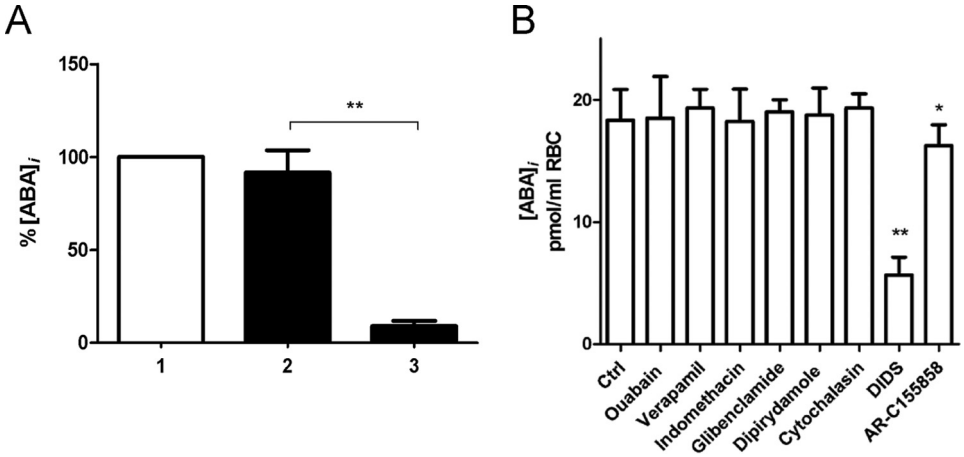

FIGURE 3. **ABA efflux from RBC and screening of ABA influx inhibitors.** *A*, RBC were incubated at a 5% hematocrit with 200 nM [^{3}H]ABA for 30 min at 22 °C and washed once at 0 °C. An aliquot of RBC suspension was counted to estimate the total intracellular ABA ([ABA]$_i$, *lane 1*). The rest of the suspension was divided into 2 aliquots and each was further washed 4 times at 0 °C (*lane 2*) or 37 °C (*lane 3*) with HBSS. The intraerythrocytic ABA concentration is expressed as percentage of the total intracellular [ABA]$_i$ (*lane 1*). **, $0.001 < p < 0.01$ compared with *white bar*, by *t* test. *B*, RBC were preincubated at a 5% hematocrit for 30 min at 37 °C without (*Ctrl*) or with each one of the compounds shown in the *abscissa*, at a 100 μM final concentration. After centrifugation and washing the pellets, cells were incubated at 22 °C with 200 nM [^{3}H]ABA for 5 min and the intracellular radioactivity was measured using a β-counter. *, $p < 0.05$ compared with control (*Ctrl*); **, $p < 0.001$ compared with Ctrl, by *t* test. Results shown are the mean ± S.D. of 3 experiments.

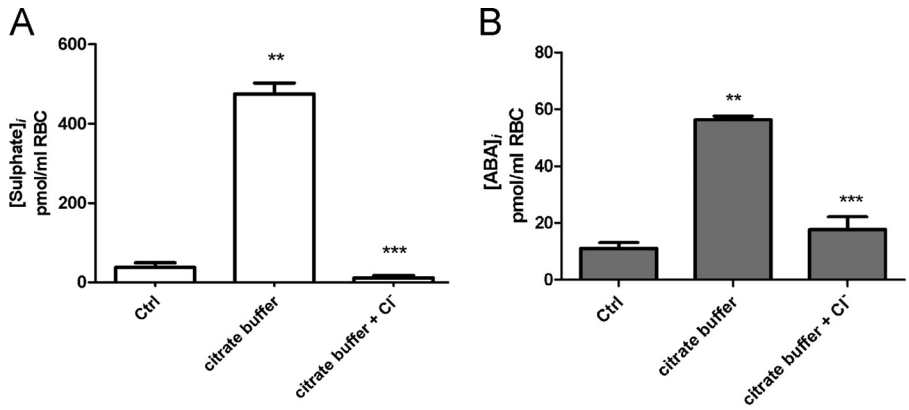

FIGURE 4. **Chloride ions compete with ABA for influx into RBC.** RBC were washed at a 5% hematocrit with HBSS (*Ctrl*) or with sodium citrate buffer. Washed cells were then resuspended in the same buffer used for washing and incubated with *A*, 3.5 μM [^{35}S]sulfate or *B*, 200 nM [^{3}H]ABA for 5 min in the presence or absence of 100 mM NaCl. After centrifugation, cells were washed in the appropriate buffer and the intracellular radioactivity was measured. **, $p < 0.05$, compared with control (*Ctrl*), by *t* test. ***, $p < 0.0001$ compared with citrate buffer. Results are the mean ± S.D. of 3 experiments.

Chloride Ions Compete with ABA for Influx in RBC—Band 3 is a monovalent anion channel, which mediates the bidirectional and electroneutral exchange of an anion with another through the plasma membrane of erythrocytes. The preferentially exchanged anions are Cl^-/HCO_3^-, but Band 3 may also exchange SO_4^{2-}/H^+ with Cl^- (35). Thus, we used [^{35}S]sulfate to study Band 3 functionality in erythrocytes. We performed experiments of [^{35}S]sulfate influx in a chloride-containing buffer (HBSS) or in a chloride-free buffer (citrate). In RBC washed and incubated with chloride-free buffer, the intracellular Cl^- content is reduced due to a net loss of Cl^- driven by the outward Cl^- gradient (36). In these conditions, the transport of [^{35}S]sulfate increased considerably, compared with its influx in RBC incubated in the same buffer supplemented with chloride or in HBSS (Fig. 4*A*). Thus, absence of competing extracellular Cl^- facilitates influx of sulfate. To verify if extracellular Cl^- was able to compete with the influx of ABA-[COO^-], influx experiments were carried out in a chloride-free buffer, supplemented or not with Cl^-. RBC were subjected to repeated washings in 80 mM Na-citrate buffer at pH 7.4, and incubated at 5% hematocrit in the presence of 100 nM [^{3}H]ABA, with or without added Cl^-. Control cells were incubated in HBSS (chloride buffer). As shown in Fig. 4*B*, influx of [^{3}H]ABA was increased in RBC resuspended in citrate buffer, and when 100 mM NaCl was added there was a significant decrease of [^{3}H]ABA influx relative to control.

Binding of Bio-ABA to Band 3—Next, we investigated whether ABA could bind to Band 3. Photochemical cross-linking of a ligand to its specific protein transporter or exchanger is frequently used to stabilize the complex and provide information difficult to obtain in a dynamic situation (37, 38). We used a biotinylated analog of ABA for binding experiments (39). In the bio-ABA molecule, the ABA moiety can be photoactivated at 254 nm (40) and can bind covalently to ABA-binding proteins, whereas the biotin moiety is detectable with the HRP-streptavidin system. The experiments were carried out on resealed ghosts that expose the extracellular side of RBC membranes (right side-out ghosts). Resealed ghosts were incubated with 100 μM bio-ABA under UV light for 5 min on ice, excess bio-ABA was removed by washing and biotinylated proteins were purified on magnetic streptavidin-coated beads, after solubilization. The samples were subjected to SDS-PAGE and Western blot, and streptavidin conjugated to horseradish peroxidase (HRP) was used for protein band detection. Bio-ABA predominantly labeled a 100-kDa band, with a shape and molecular size similar to Band 3 (Fig. 5*A*, *lane 1*). To confirm that the 100-kDa band was indeed Band 3, the same membrane was also stained with streptavidin-HRP or with a mAb against Band 3 (Fig. 5*A*, *lane 2*). The specificity of the binding between

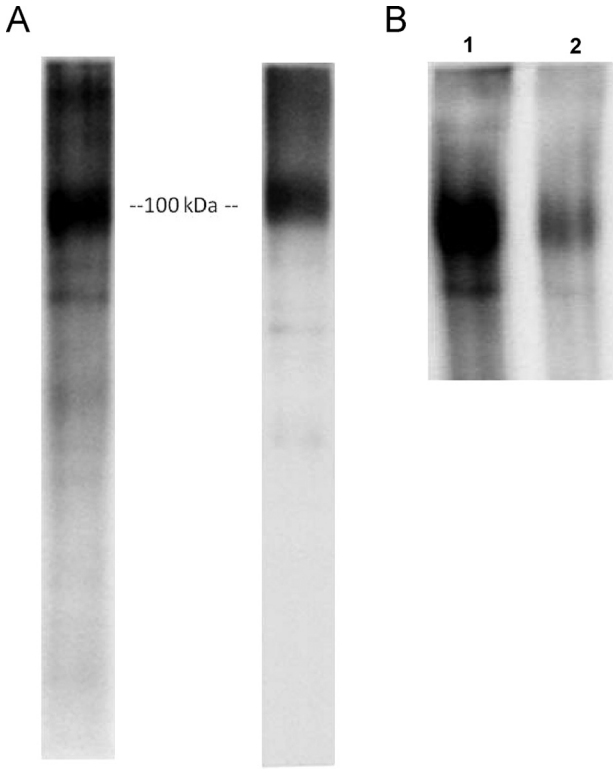

FIGURE 5. **Band 3 from RBC ghosts binds bio-ABA.** Resealed ghosts were incubated with 100 μM bio-ABA for 3 h at 22 °C. After UV irradiation (0.4 Joules for 5 min), ghosts were washed and solubilized, and bio-ABA-binding proteins were purified using streptavidin-coated beads and subjected to SDS-PAGE and Western blot. *A*, a representative nitrocellulose membrane stained with streptavidin-HRP (*lane 1*), or with a monoclonal anti-Band 3 antibody (*lane 2*). *B*, a representative nitrocellulose membrane from an incubation of resealed ghosts with bio-ABA, without (*lane 1*), or with excess unlabeled ABA (*lane 2*), stained with an anti-Band 3 monoclonal antibody.

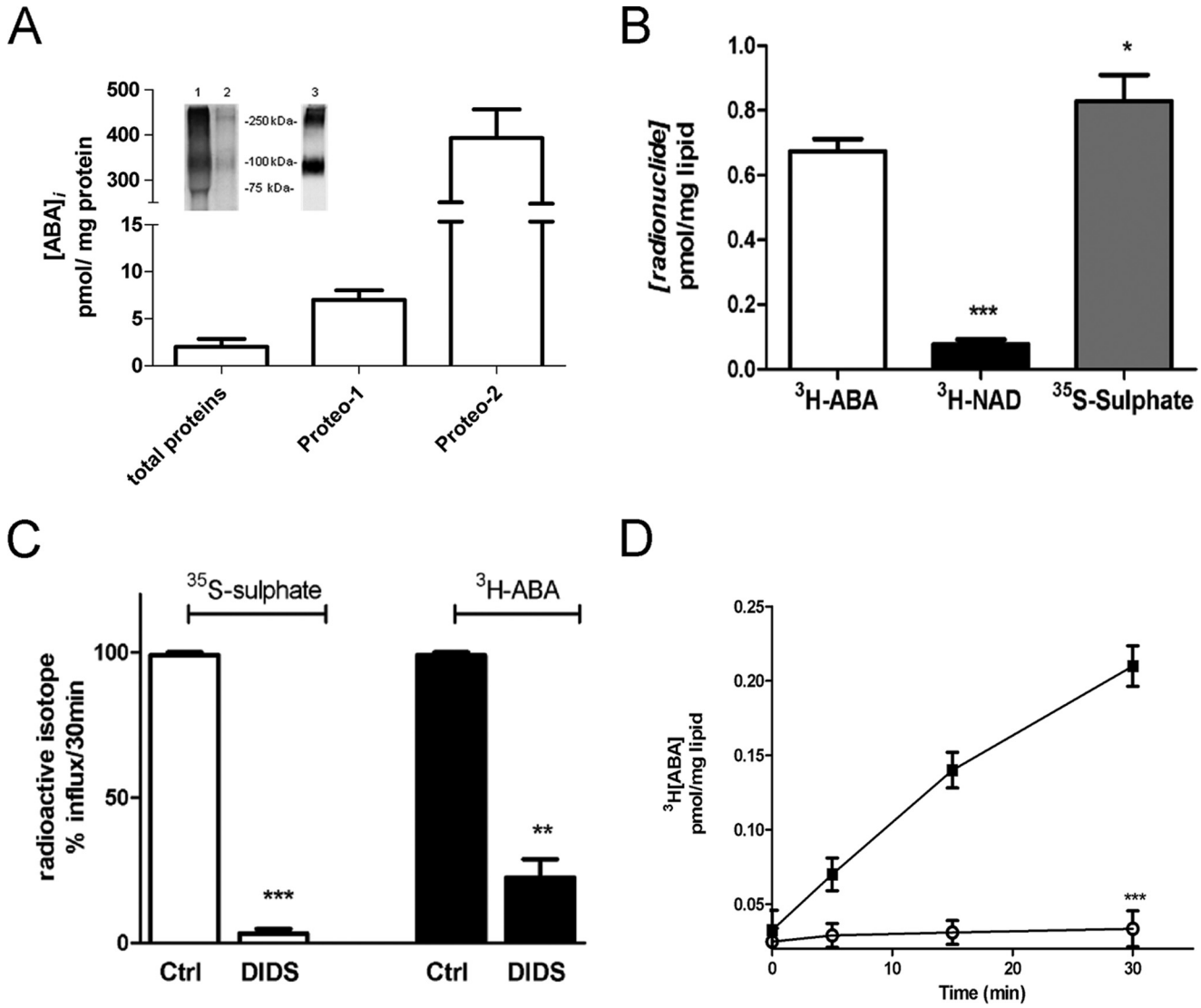

FIGURE 6. **Purification, reconstitution of Band 3, and ABA transport in liposomes and proteoliposomes.** *A,* [^{3}H]ABA uptake by proteoliposomes reconstituted with total ghost proteins, or with proteins eluted from a DE-52 column with 1 M NaCl (*Proteo-1*) or 1.5 M NaCl (*Proteo-2*). The proteoliposomes were incubated with 100 nM [^{3}H]ABA for 30 min at 22 °C; samples were then filtered on glass fiber paper as described under "Experimental Procedures" and the radioactivity of the filter was measured in a β-counter. Results are the mean ± S.D. of 4 experiments. The *inset* shows an SDS-PAGE separation stained with ProSieve Blu Protein Staining of 10 μg of solubilized ghost proteins eluted from a DE-52 column with 1 M NaCl (*lane 1*) or 1.5 M NaCl (*lane 2*). Western blot of 1 μg of the same sample loaded in *lane 2*, probed with an anti-Band 3 monoclonal antibody (*lane 3*). *B,* Proteo-2 liposomes were incubated for 30 min at 22 °C with 500 nM [^{3}H]ABA, 500 nM [^{3}H]NAD, or 3.5 μM [^{35}S]sulfate. ***, $p < 0.001$; *, $0.001 < p < 0.01$ compared with *white bar*, by *t* test. *C*, proteoliposomes reconstituted with Band 3 purified from ghosts pretreated, or not (*Ctrl*), with 100 μM DIDS were incubated for 30 min with 100 nM [^{3}H]ABA or 3.5 μM [^{35}S]sulfate. ***, $p < 0.001$; **, $p < 0.05$ compared with the respective control (*Ctrl*) by *t* test. *D,* time course of ABA influx in proteo-2 (*black squares*) and in liposomes (*open circles*) that were incubated with 100 nM [^{3}H]ABA for 0, 5, 15, and 30 min at 22 °C. At the times indicated, incubation samples were filtered on glass fiber filters, washed in isotonic buffer, and the incorporated radioactivity was measured with a β-counter. ***, $p < 0.001$ compared with proteo-2, by *t* test (mean ± S.D. from $n = 3$ experiments).

Band 3 and ABA was demonstrated by displacement of bio-ABA by excess non-biotinylated ABA (Fig. 5*B*, *lane 2*).

ABA Transport Occurs Across Band 3-reconstituted Proteoliposomes—Under physiological conditions, Band 3 is present in dimeric and tetrameric forms in erythrocyte membranes (41). Moreover, it has been previously demonstrated that treatment with OG induces Band 3 aggregation into high molecular weight oligomers, without significant modification of the protein secondary structure (42). Indeed, SDS-PAGE of OG-solubilized, purified Band 3, shows a predominant band at 100 kDa (corresponding to the monomer) and another at 250 kDa, corresponding to dimers (Fig. 6*A*). After removal of the peripheral proteins, Band 3 was purified from human erythrocyte ghosts solubilized in 1% OG by anion exchange chromatography. Fig. 6*A* shows the SDS-PAGE and Western blot of the final purification steps: the 1 M NaCl eluate, containing Band 3 along with several contaminating proteins, and the 1.5 M NaCl eluate, containing highly purified Band 3, both in monomeric and dimeric forms. Reconstitution of proteoliposomes with total erythrocyte ghost proteins, or with the 1 and 1.5 M NaCl eluates from the DE-52 column, showed a progressive increase of [^{3}H]ABA influx along with the enrichment of Band 3 (Fig. 6*A*). To verify the functional activity of reconstituted Band 3, we compared the influx of ABA into proteoliposomes reconstituted with

purified Band 3 with the influx of [^{3}H]NAD and [^{35}S]sulfate, taken as negative and positive controls, respectively (Fig. 6*B*). No transport whatsoever of [^{3}H]NAD (nor of [^{14}C]glucose, data not shown) was detectable with the same Band 3-reconstituted proteoliposomes, which conversely did transport labeled sulfate, as well as ABA. To inhibit Band 3 transport, white ghosts were treated with 100 μM DIDS for 30 min, allowing the irreversible binding of DIDS to Band 3. Band 3 was then purified and reconstituted into proteoliposomes, as described under "Experimental Procedures." Fig. 6*C* shows that the transport of labeled sulfate and ABA in proteoliposomes reconstituted with purified Band 3 pre-treated with DIDS is strongly reduced compared with the control. These results indicate that reconstitution of Band 3 into proteoliposomes restores a functional Band 3, capable of transporting sulfate and ABA, and that DIDS inhibits both the transport of sulfate and that of ABA.

To evaluate the extent of a nonspecific adsorption of ABA to the lipid bilayer, liposomes prepared with or without purified Band 3 were incubated with 100 nM [^{3}H]ABA. As shown in Fig. 6*D*, the concentration of intravesicular ABA in the proteoliposomes reached 0.2 pmol/mg of lipid in 30 min. Conversely, the amount of ABA associated with liposomes was considerably lower (about 0.02 pmol/mg lipid) and did not increase with incubation time. The ~0.1% fraction of total ABA present at pH 7.4 in the protonated form (ABA-COOH), which can diffuse through the lipid bilayer, as already demonstrated in higher plants (43), could account for this low amount of lipid-associated ABA.

ABA Stimulates ATP Release from RBC via Activation of Adenylate Cyclase—Erythrocyte stress is known to modulate vascular tone by inducing the release of ATP from intact RBC via the activation of adenylate cyclase (AC) and the consequent increase of the intraerythrocytic cAMP concentration $[cAMP]_i$ (44, 45). ABA is known to activate AC and induce an increase of $[cAMP]_i$ in several nucleated cell types, including human granulocytes (12), the rat insulinoma cells RIN-m and INS-1 (17, 18), and aortic endothelial cells (46). Thus, we first investigated whether ABA influx into RBC induced an increase of the $[cAMP]_i$.

The $[cAMP]_i$ increased by 100 ± 10% in RBC incubated for 5 min with 0.1 μM ABA, as compared with untreated cells (Fig. 7*A*). It was previously demonstrated that a synthetic ABA analog, compound #10, which inhibits the ABA-triggered increase of $[cAMP]_i$ in human granulocytes, competes with ABA for binding to LANCL2 and inhibits the functional activation of granulocytes induced by exogenous ABA (29). We observed that analog #10 was indeed able to inhibit the $[cAMP]_i$ increase induced by ABA in erythrocytes, indicating that LANCL2 is involved in the intraerythrocytic activation of AC by extracellular ABA (Fig. 7*A*). Preincubation of RBC with DIDS prevented the increase of the $[cAMP]_i$ in the presence of ABA (Fig. 7*A*), confirming that a functional Band 3 is required for ABA influx and AC activation. No effect of DIDS or of compound #10 on cAMP levels was observed in RBC incubated without ABA (data not shown).

We then addressed the question of whether ABA could induce ATP release from intact erythrocytes. To this purpose, we preliminarily tested whether ABA could cause hemolysis. Erythrocyte suspensions (250 μl), without (control) or with increasing ABA concentrations (from 0.1 μM to 1 mM), were incubated for 20 min at 22 °C, centrifuged for 30 s at 16,000 × *g*, and the absorbance of the supernatants was measured at 405 nm. No difference was observed between control and ABA-containing incubations, allowing the conclusion that ABA does not induce RBC lysis over the concentration range tested. Thus, RBC were incubated at a hematocrit of 0.05% without (control) or with increasing ABA concentrations and ATP release was measured after 0 and 20 min. Fig. 7*B* shows that 0.1 μM ABA was sufficient to induce ATP release from erythrocytes.

Finally, we investigated the possible causal role of AC activation in the ABA-induced ATP release by inhibiting the generation of cyclic AMP with the adenylate cyclase inhibitor dideoxyadenosine, or with the PKA-specific myristoylated peptide inhibitor (I-PKA). As shown in Fig. 7*C*, both dideoxyadenosine and I-PKA inhibited the ABA-triggered ATP release from intact RBC, indicating a causal role of the $[cAMP]_i$ increase in the ABA-induced ATP efflux.

Discussion

In the present study, we show for the first time that an ABA transport is present in human erythrocytes. RBC represent a convenient model system for the study of ABA transport in mammalian cells, for two reasons: (i) RBC plasma membranes (ghosts) can be easily isolated and resealed, yielding transport-competent vesicles (47), and (ii) RBC express the ABA receptor LANCL2, which upon ABA binding stimulates AC in several animal cell types (12–18, 48), thus triggering the first step of the intracellular ABA signaling pathway after ABA influx. The first member of the LANCL family, LANCL1, was indeed isolated from human erythrocyte membranes, where it is present as a peripheral membrane protein (49). Our results demonstrate that LANCL2 is present in RBC ghosts, as detected by Western blot with a LANCL2-specific monoclonal antibody, and is a peripheral membrane protein. Because LANCL2 is located on the intracellular side of the plasmamembrane, an ABA transport system is required to allow the extracellular hormone to cross the plasma membrane and bind to its receptor.

The results obtained in this study demonstrate that transport of ABA indeed occurs across both RBC membranes and resealed ghosts and that removal of LANCL2, by means of chemical treatments in the absence of detergents, does not affect ABA transport, indicating that LANCL2 is neither necessary nor adjuvant for ABA influx into RBC.

The ABA transporter in RBC is identified as the anion transporter Band 3 on the basis of the following results: (i) proteoliposomes reconstituted with purified Band 3 are able to transport ABA and sulfate, and (ii) the specific Band 3 inhibitor DIDS inhibits influx of ABA. The fact that Band 3 binds bio-ABA and bio-ABA can be displaced by excess ABA confirms that a specific interaction occurs between ABA and the transporter.

Band 3 exhibits half-saturation at chloride concentrations of ~45 mM, both in intact RBC and in RBC ghosts (50, 51). Thus, it may not be surprising that saturation of ABA transport was not observed up to ABA concentrations of 25 mM.

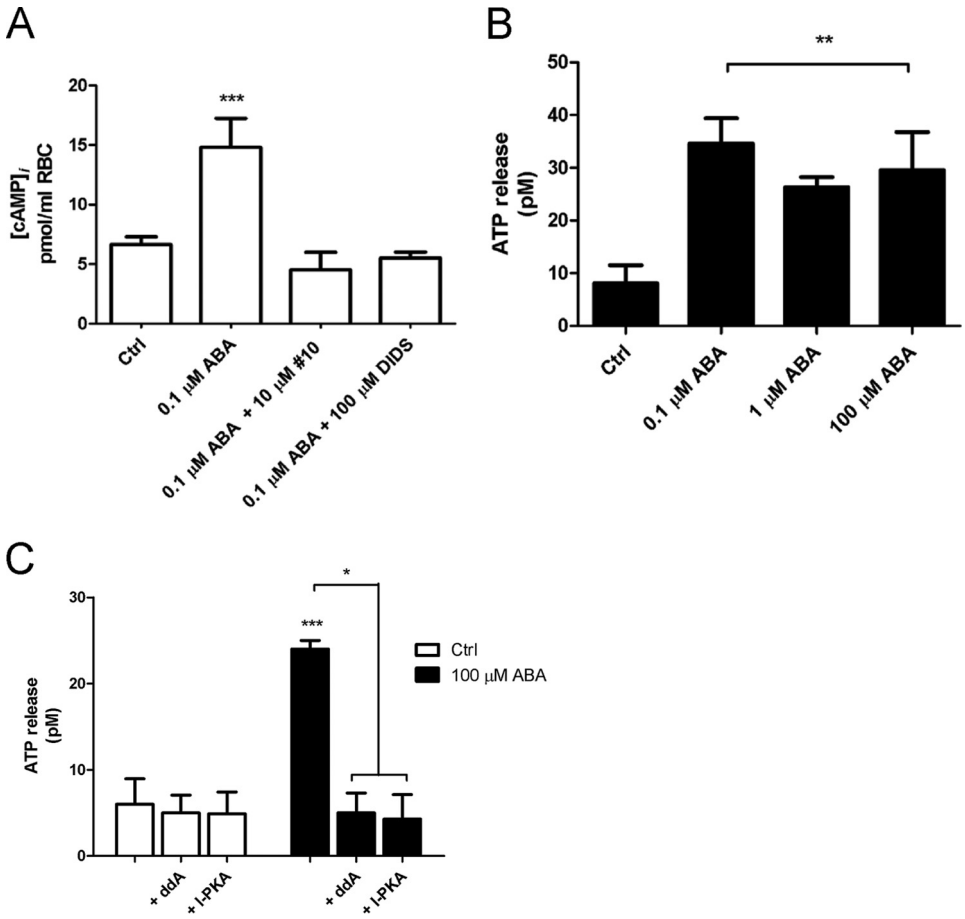

FIGURE 7. **The ABA antagonist #10 and Band 3 inhibitor DIDS inhibit the ABA-induced $[cAMP]_i$ rise and ATP release.** *A,* RBC were preincubated at a 50% hematocrit with 250 μM of the cAMP phosphodiesterase inhibitor 3-isobutyl-1-methylxanthine for 15 min; cells were then incubated at 22 °C for 5 min without (*Ctrl*) or with 0.1 μM ABA, without or with 10 μM #10 or 100 μM DIDS. The intraerythrocytic cAMP concentrations were measured as described under "Experimental Procedures." ***, $p < 0.03$ compared with control (*Ctrl*). *B,* erythrocytes were incubated at a 0.05% hematocrit without or with 0.1, 1.0, or 100 μM ABA for 20 min and ATP released from the intact RBC was then determined as described under "Experimental Procedures." **, $p < 0.01$ compared with control (*Ctrl*). *C,* RBC were preincubated for 15 min at 37 °C at a 0.05% hematocrit without or with 100 μM 2′,3′-dideoxyadenosine (*ddA*), a specific adenylate cyclase inhibitor, or with 10 μM of a specific myristoylated peptide inhibitor of PKA (*I-PKA*). RBC were then incubated without or with 100 μM ABA for 20 min at 22 °C. Cells were centrifuged and ATP content in the supernatant was measured as described under "Experimental Procedures." Results are expressed as the difference between the ATP concentration measured after 20 min incubation and the ATP concentration at time 0. ***, $p < 0.001$ compared with control (*Ctrl*); *, $p < 0.05$ compared with 100 μM ABA, by *t* test (mean ± S.D., $n = 3$ experiments).

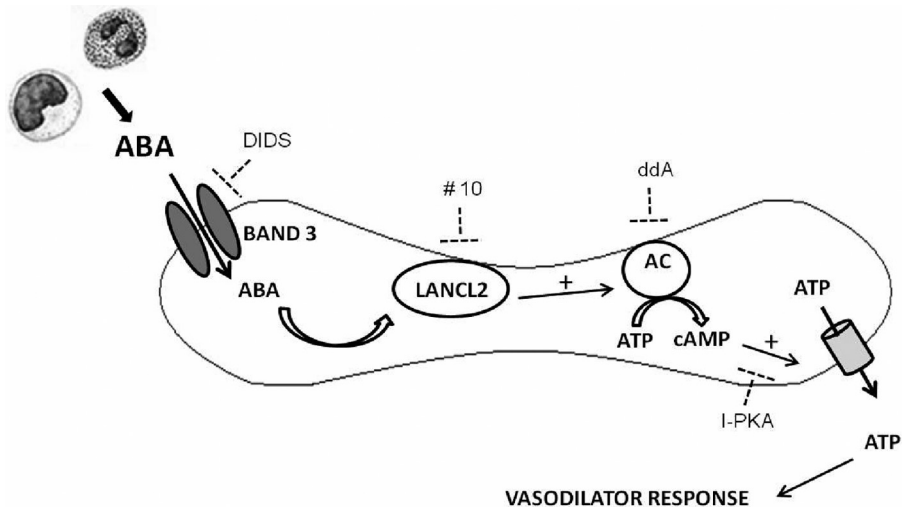

FIGURE 8. **Schematic representation of the ABA-induced $[cAMP]_i$ increase and ATP release.** In the microcirculation, paracrine ABA produced by inflammatory cells enters into RBC across Band 3. Intracellular ABA binds and activates the LANCL2 receptor with consequent activation of AC and overproduction of cAMP. Downstream of the cAMP increase, ATP is released from erythrocytes. Specific inhibitors of the ABA signaling pathway are indicated by *dashed arrows*. *DIDS*, a Band 3 inhibitor; *#10*, a synthetic ABA antagonist of the LANCL2 receptor; *ddA*, a adenylate cyclase inhibitor; *I-PKA*, a PKA-specific myristoylated peptide inhibitor.

Protonated ABA can diffuse through the lipid bilayer (43); however, a very low percentage of ABA is protonated at the near-neutral pH present in animal fluids and tissues, making the presence of a transport system essential for ABA trafficking between intra and extracellular fluids.

Once internalized in RBC, ABA induces intracellular cAMP formation, leading to a regulated release of ATP (Fig. 8). The following events are required for intraerythrocytic activation of AC to occur, with consequent $[cAMP]_i$ increase: (i) ABA transport through Band 3, as demonstrated by inhibition of the $[cAMP]_i$ increase by DIDS, and (ii) ABA binding to and activation of LANCL2, as demonstrated by inhibition of the $[cAMP]_i$ increase by the ABA antagonist analog #10. It has been previously reported that in erythrocytes a $[cAMP]_i$ increase induces ATP release through two different mechanisms: (i) via pannexin 1, in response to RBC exposure to low O_2 or (ii) via VDAC channels, in response to β-adrenergic receptor activation (45). It can be hypothesized that ABA released from activated inflammatory cells (granulocytes, monocytes, microglia) and/or from vascular smooth muscle cells could locally reach concentrations in the 100 nM range (up from 1 to 10 nM basal plasma values) (52) in the microcirculation.

ABA concentrations in the 10–100 nM range were indeed measured in human atherosclerotic plaques (13). Moreover, based on the amount of ABA that can be released by activated human monocytes (13), an ABA concentration of 100 nM could be attained locally by $\sim 8 \times 10^6$ cells, extravasated in a volume of 400 μl. This monocyte density can be easily reached under inflammatory tissue conditions (53, 54). As summarized in Fig. 8, extracellular ABA could then trigger a cAMP-dependent ATP release from erythrocytes, thus contributing to the vasodilator response to local inflammation.

In nucleated cells, Band 3 (SLC4A1/AE1) is present along with two other anion transporters, SLC4A2/AE2 and SLC4A3/AE3 (55). Whether in these cells AE1 alone, or all three transporters are capable of ABA transport remains to be established.

References

1. Nambara, E., and Marion-Poll, A. (2005) Abscisic acid biosynthesis and catabolism. *Annu. Rev. Plant Biol.* **56,** 165–185
2. Xue-Xuan, X., Hong-Bo, S., Yuan-Yuan, M., Gang, X., Jun-Na, S., Dong-Gang, G., and Cheng-Jiang, R. (2010) Biotechnological implications from abscisic acid (ABA) roles in cold stress and leaf senescence as an important signal for improving plant sustainable survival under abiotic-stressed conditions. *Crit. Rev. Biotechnol.* **30,** 222–230
3. Guo, J., Yang, X., Weston, D. J., and Chen, J. G. (2011) Abscisic acid receptors: past, present and future. *J. Integr. Plant Biol.* **53,** 469–479
4. Raghavendra, A. S., Gonugunta, V. K., Christmann, A., and Grill, E. (2010) ABA perception and signalling. *Trends Plant Sci.* **15,** 395–401
5. Joshi-Saha, A., Valon, C., and Leung, J. (2011) A brand new START: abscisic acid perception and transduction in the guard cell. *Sci. Signal.* **4,** re4
6. Kang, J., Hwang, J. U., Lee, M., Kim, Y. Y., Assmann, S. M., Martinoia, E., and Lee, Y. (2010) PDR-type ABC transporter mediates cellular uptake of the phytohormone abscisic acid. *Proc. Natl. Acad. Sci. U.S.A.* **107,** 2355–2360
7. Kuromori, T., and Shinozaki, K. (2010) ABA transport factors found in *Arabidopsis* ABC transporters. *Plant Signal. Behav.* **5,** 1124–1126
8. Kanno, Y., Hanada, A., Chiba, Y., Ichikawa, T., Nakazawa, M., Matsui, M., Koshiba, T., Kamiya, Y., and Seo, M. (2012) Identification of an abscisic acid transporter by functional screening using the receptor complex as a sensor. *Proc. Natl. Acad. Sci. U.S.A.* **109,** 9653–9658
9. Zhang, H., Zhu, H., Pan, Y., Yu, Y., Luan, S., and Li, L. (2014) A DTX/MATE-type transporter facilitates abscisic acid efflux and modulates ABA sensitivity and drought tolerance in *Arabidopsis*. *Mol Plant.* **7,** 1522–1532
10. Li, H. H., Hao, R. L., Wu, S. S., Guo, P. C., Chen, C. J., Pan, L. P., and Ni, H. (2011) Occurrence, function and potential medicinal applications of the phytohormone abscisic acid in animals and humans. *Biochem. Pharmacol.* **82,** 701–712
11. Bruzzone, S., Ameri, P., Sturla, L., Guida, L., De Flora, A., and Zocchi, E. (2012) Abscisic acid: a new mammalian hormone regulating glucose homeostasis. *Messenger* **1,** 141–149
12. Bruzzone, S., Moreschi, I., Usai, C., Guida, L., Damonte, G., Salis, A., Scarfì, S., Millo, E., De Flora, A., and Zocchi, E. (2007) Abscisic acid is an endogenous cytokine in human granulocytes with cyclic ADP-ribose as second messenger. *Proc. Natl. Acad. Sci. U.S.A.* **104,** 5759–5764
13. Magnone, M., Bruzzone, S., Guida, L., Damonte, G., Millo, E., Scarfì, S., Usai, C., Sturla, L., Palombo, D., De Flora, A., and Zocchi, E. (2009) Abscisic acid released by human monocytes activates monocytes and vascular smooth muscle cell responses involved in atherogenesis. *J. Biol. Chem.* **284,** 17808–17818
14. Bodrato, N., Franco, L., Fresia, C., Guida, L., Usai, C., Salis, A., Moreschi, I., Ferraris, C., Verderio, C., Basile, G., Bruzzone, S., Scarfì, S., De Flora, A., and Zocchi, E. (2009) Abscisic acid activates the murine microglial cell line N9 through the second messenger cyclic ADP-ribose. *J. Biol. Chem.* **284,** 14777–14787
15. Scarfì, S., Ferraris, C., Fruscione, F., Fresia, C., Guida, L., Bruzzone, S., Usai, C., Parodi, A., Millo, E., Salis, A., Burastero, G., De Flora, A., and Zocchi, E. (2008) Cyclic ADP-ribose-mediated expansion and stimulation of human mesenchymal stem cells by the plant hormone abscisic acid. *Stem Cells* **26,** 2855–2864
16. Scarfì, S., Fresia, C., Ferraris, C., Bruzzone, S., Fruscione, F., Usai, C., Benvenuto, F., Magnone, M., Podestà, M., Sturla, L., Guida, L., Albanesi, E., Damonte, G., Salis, A., De Flora, A., and Zocchi, E. (2009) The plant hormone abscisic acid stimulates the proliferation of human hemopoietic progenitors through the second messenger cyclic ADP-ribose. *Stem Cells* **27,** 2469–2477
17. Bruzzone, S., Bodrato, N., Usai, C., Guida, L., Moreschi, I., Nano, R., Antonioli, B., Fruscione, F., Magnone, M., Scarfì, S., De Flora, A., and Zocchi, E. (2008) Abscisic acid is an endogenous stimulator of insulin release from human pancreatic islets with cyclic ADP ribose as second messenger. *J. Biol. Chem.* **283,** 32188–32197
18. Sturla, L., Fresia, C., Guida, L., Bruzzone, S., Scarfì, S., Usai, C., Fruscione, F., Magnone, M., Millo, E., Basile, G., Grozio, A., Jacchetti, E., Allegretti, M., De Flora, A., and Zocchi, E. (2009) LANCL2 is necessary for abscisic acid binding and signaling in human granulocytes and in rat insulinoma cells. *J. Biol. Chem.* **284,** 28045–28057
19. Lu, P., Bevan, D. R., Lewis, S. N., Hontecillas, R., and Bassaganya-Riera, J. (2011) Molecular modeling of lanthionine synthetase component C-like protein 2: a potential target for the discovery of novel type 2 diabetes prophylactics and therapeutics. *J. Mol. Model.* **17,** 543–553
20. Sturla, L., Fresia, C., Guida, L., Grozio, A., Vigliarolo, T., Mannino, E., Millo, E., Bagnasco, L., Bruzzone, S., De Flora, A., and Zocchi, E. (2011) Binding of abscisic acid to human LANCL2. *Biochem. Biophys. Res. Commun.* **415,** 390–395
21. Landlinger, C., Salzer, U., and Prohaska, R. (2006) Myristoylation of human LanC-like protein 2 (LANCL2) is essential for the interaction with the plasma membrane and the increase in cellular sensitivity to adriamycin. *Biochim. Biophys. Acta* **1758,** 1759–1767
22. Moriya, K., Nagatoshi, K., Noriyasu, Y., Okamura, T., Takamitsu, E., Suzuki, T., and Utsumi, T. (2013) Protein *N*-myristoylation plays a critical role in the endoplasmic reticulum morphological change induced by overexpression of protein Lunapark, an integral membrane protein of the endoplasmic reticulum. *PLoS One* **8,** e78235
23. Yamazaki, D., Yoshida, S., Asami, T., and Kuchitsu, K. (2003) Visualization of abscisic acid-perception sites on the plasma membrane of stomatal guard cells. *Plant J.* **35,** 129–139
24. Ey, P. L., Prowse, S. J., and Jenkin, C. R. (1978) Isolation of pure IgG1, IgG2a and IgG2b immunoglobulins from mouse serum using protein A-Sepharose. *Immunochemistry* **15,** 429–436
25. Bradford, M. M. (1976) A rapid and sensitive method for the quantitation

of microgram quantities of protein utilizing the principle of protein-dye binding. *Anal. Biochem.* **72,** 248–254
26. Franco, L., Guida, L., Bruzzone, S., Zocchi, E., Usai, C., and De Flora, A. (1998) The transmembrane glycoprotein CD38 is a catalytically active transporter responsible for generation and influx of the second messenger cyclic ADP-ribose across membranes. *FASEB J.* **12,** 1507–1520
27. Le Page-Degivry, M. T., Bidard, J. N., Rouvier, E., Bulard, C., and Lazdunski, M. (1986) Presence of abscisic acid, a phytohormone, in the mammalian brain. *Proc. Natl. Acad. Sci. U.S.A.* **83,** 1155–1158
28. Lowry, O. H., Rosebrough, N. J., Farr, A. L., and Randall, R. J. (1951) Protein measurement with the Folin phenol reagent. *J. Biol. Chem.* **193,** 265–275
29. Grozio, A., Millo, E., Guida, L., Vigliarolo, T., Bellotti, M., Salis, A., Fresia, C., Sturla, L., Magnone, M., Galatini, A., Damonte, G., De Flora, A., Bruzzone, S., Bagnasco, L., and Zocchi, E. (2011) Functional characterization of a synthetic abscisic acid analog with anti-inflammatory activity on human granulocytes and monocytes. *Biochem. Biophys. Res. Commun.* **415,** 696–701
30. Pedemonte, C. H., and Kaplan, J. H. (1988) Inhibition and derivatization of the renal Na,K-ATPase by dihydro-4,4′-diisothiocyanatostilbene-2,2′-disulfonate. *Biochemistry* **27,** 7966–7973
31. Gatto, C., Lutsenko, S., and Kaplan, J. H. (1997) Chemical modification with dihydro-4,4′-diisothiocyanostilbene-2,2′-disulfonate reveals the distance between K480 and K501 in the ATP-binding domain of the Na,K-ATPase. *Arch. Biochem. Biophys.* **340,** 90–100
32. Niggli, V., Sigel, E., and Carafoli, E. (1982) Inhibition of the purified and reconstituted calcium pump of erythrocytes by micro M levels of DIDS and NAP-taurine. *FEBS Lett.* **138,** 164–166
33. Ruetz, S., Hugentobler, G., and Meier, P. J. (1988) Functional reconstitution of the canalicular bile salt transport system of rat liver. *Proc. Natl. Acad. Sci. U.S.A.* **85,** 6147–6151
34. Poole, R. C., and Halestrap, A. P. (1991) Reversible and irreversible inhibition, by stilbenedisulphonates, of lactate transport into rat erythrocytes. Identification of some new high-affinity inhibitors. *Biochem. J.* **275,** 307–312
35. Jennings, M. L. (1976) Proton fluxes associated with erythrocyte membrane anion exchange. *J Membr Biol.* **28,** 187–205
36. Jennings, M. L. (2005) Evidence for a second binding/transport site for chloride in erythrocyte anion transporter AE1 modified at glutamate 681. *Biophys. J.* **88,** 2681–2691
37. Mizutani, M., Mukaiyama, K., Xiao, J., Mori, M., Satou, R., Narita, S., Okuda, S., and Tokuda, H. (2013) Functional differentiation of structurally similar membrane subunits of the ABC transporter LolCDE complex. *FEBS Lett.* **587,** 23–29
38. Kawaguchi, Y., Tanaka, G., Nakase, I., Imanishi, M., Chiba, J., Hatanaka, Y., and Futaki, S. (2013) Identification of cellular proteins interacting with octaarginine (R8) cell-penetrating peptide by photo-crosslinking. *Bioorg. Med. Chem. Lett.* **23,** 3738–3740
39. Grozio, A., Gonzalez, V. M., Millo, E., Sturla, L., Vigliarolo, T., Bagnasco, L., Guida, L., D'Arrigo, C., De Flora, A., Salis, A., Martin, E. M., Bellotti, M., and Zocchi, E. (2013) Selection and characterization of single stranded DNA aptamers for the hormone abscisic acid. *Nucleic Acid Ther.* **23,** 322–331
40. Wu, Z. Y., Chen, J., and Zhu, M. J. (1996) Identification of the photoaffinity-labeled abscisic acid binding proteins from maize root microsome. *Sheng Wu Hua Xue Yu Sheng Wu Wu Li Xue Bao* (*Shanghai*) **28,** 694–696
41. Jennings, M. L., and Nicknish, J. S. (1984) Erythrocyte band 3 protein: evidence for multiple membrane-crossing segments in the 17,000-dalton chymotryptic fragment. *Biochemistry* **23,** 6432–6436
42. Werner, P. K., and Reithmeier, R. A. (1985) Molecular characterization of the human erythrocyte anion transport protein in octyl glucoside. *Biochemistry* **24,** 6375–6381
43. Boursiac, Y., Léran, S., Corratgé-Faillie, C., Gojon, A., Krouk, G., and Lacombe, B. (2013) ABA transport and transporters. *Trends Plant Sci.* **18,** 325–333
44. Montalbetti, N., Leal Denis, M. F., Pignataro, O. P., Kobatake, E., Lazarowski, E. R., and Schwarzbaum, P. J. (2011) Homeostasis of extracellular ATP in human erythrocytes. *J. Biol. Chem.* **286,** 38397–38407
45. Ellsworth, M. L., and Sprague, R. S. (2012) Regulation of blood flow distribution in skeletal muscle: role of erythrocyte-released ATP. *J. Physiol.* **590,** 4985–4991
46. Guri, A. J., Misyak, S. A., Hontecillas, R., Hasty, A., Liu, D., Si, H., and Bassaganya-Riera, J. (2010) Abscisic acid ameliorates atherosclerosis by suppressing macrophage and $CD4^+$ T cell recruitment into the aortic wall. *J. Nutr. Biochem.* **21,** 1178–1185
47. Bruzzone, S., Guida, L., Zocchi, E., Franco, L., and De Flora, A. (2001) Connexin 43 hemi channels mediate Ca^{2+}-regulated transmembrane NAD^+ fluxes in intact cells. *FASEB J.* **15,** 10–12
48. De Flora, A., Bruzzone, S., Guida, L., Sturla, L., Magnone, M., Fresia, C., Vigliarolo, T., Mannino, E., Sociali, G., and Zocchi, E. (2014) Toward a medicine-oriented use of human hormone/nutritional supplement abscisic acid. *Messenger* **3,** 1–12
49. Mayer, H., Breuss, J., Ziegler, S., and Prohaska, R. (1998) Molecular characterization and tissue-specific expression of a murine putative G-protein-coupled receptor. *Biochim. Biophys. Acta* **1399,** 51–56
50. Liu, D., Kennedy, S. D., and Knauf, P. A. (1996) Source of transport site asymmetry in the band 3 anion exchange protein determined by NMR measurements of external Cl^- affinity. *Biochemistry.* **35,** 15228–15235
51. Falke, J. J., Pace, R. J., and Chan, S. I. (1984) Chloride binding to the anion transport binding sites of band 3. A ^{35}Cl NMR study. *J. Biol. Chem.* **259,** 6472–6480
52. Bruzzone, S., Ameri, P., Briatore, L., Mannino, E., Basile, G., Andraghetti, G., Grozio, A., Magnone, M., Guida, L., Scarfì, S., Salis, A., Damonte, G., Sturla, L., Nencioni, A., Fenoglio, D., Fiory, F., Miele, C., Beguinot, F., Ruvolo, V., Bormioli, M., Colombo, G., Maggi, D., Murialdo, G., Cordera, R., De Flora, A., and Zocchi, E. (2012) The plant hormone abscisic acid increases in human plasma after hyperglycemia and stimulates glucose consumption by adipocytes and myoblasts. *FASEB J.* **26,** 1251–1260
53. Schubert, K., Polte, T., Bönisch, U., Schader, S., Holtappels, R., Hildebrandt, G., Lehmann, J., Simon, J. C., Anderegg, U., and Saalbach, A. (2011) Thy-1 (CD90) regulates the extravasation of leukocytes during inflammation. *Eur. J. Immunol.* **41,** 645–656
54. Badrnya, S., Schrottmaier, W. C., Kral, J. B., Yaiw, K. C., Volf, I., Schabbauer, G., Söderberg-Nauclér, C., and Assinger, A. (2014) Platelets mediate oxidized low-density lipoprotein-induced monocyte extravasation and foam cell formation. *Arterioscler. Thromb. Vasc. Biol.* **34,** 571–580
55. Romero, M. F., Fulton, C. M., and Boron, W. F. (2004) The SLC4 family of HCO_3^- transporters. *Pflugers Arch.* **447,** 495–509

Abscisic Acid Transport in Human Erythrocytes

Tiziana Vigliarolo, Lucrezia Guida, Enrico Millo, Chiara Fresia, Emilia Turco, Antonio De Flora and Elena Zocchi

J. Biol. Chem. 2015, 290:13042-13052.
doi: 10.1074/jbc.M114.629501 originally published online April 6, 2015
